


Cite this: *RSC Adv.*, 2025, 15, 38056

# Structure–property relationships of flexible, non-isocyanate polyurethane foams from lignin and castor oil-based reagents

Kathryn Evancho,<sup>a</sup> Richard S. Reiner,<sup>b</sup> Biljana M. Bujanovic,<sup>c</sup> Srikanth Pilla<sup>d</sup> \*<sup>cdef</sup> and James Sternberg<sup>e</sup> \*<sup>a</sup>

Polyurethane foam is a valuable material with applications across the automotive, packaging, construction, appliance, and furniture industries. However, traditional polyurethane foams are made from petroleum-based precursors including harmful isocyanates. Isocyanates are the leading cause of workplace asthma and are made from toxic phosgene gas, representing a challenge to green chemistry principles. To address these concerns, non-isocyanate polyurethane (NIPU) foams replace the traditional polyurethane reaction with a safer, non-isocyanate process most often employing cyclic carbonates and diamines. Current approaches to NIPU foams struggle to meet the low-density and flexibility of commercial foams and also employ many petroleum-derived and toxic agents. This work demonstrates the use of kraft lignin, a crosslinked aromatic polymer produced by the dominant kraft pulping process, as an effective raw material for flexible NIPU foams, reaching densities below 100 kg m<sup>-3</sup> while displaying flexible compression properties. A biobased, aliphatic agent was added in various amounts to introduce flexibility to the polymer structure while modifying the viscosity of the reaction mixture to enable increased rise height of foams containing over 30% lignin. The thermal, mechanical, and burn testing results of a series of NIPU foams are compared to a conventional PU reference foam and the structure–property relationships of the novel materials are explored based on the lignin-to-aliphatic carbon content. The results show a fully biobased, flexible, NIPU foam from lignin that can approach commercial properties, helping to demonstrate the relevance of NIPU foams for many applications.

Received 31st July 2025  
Accepted 9th September 2025

DOI: 10.1039/d5ra05582b

rsc.li/rsc-advances

## Introduction

Plastics are a versatile material that are heavily relied upon in our modern society. It is estimated that 400 million tons of plastic are produced globally per year.<sup>1</sup> Plastics are far from harmless; they pose significant threats to both environment and human health.<sup>2</sup> One threat lies in the production step of a plastic's life-cycle. Plastics are produced from primarily petroleum-based and often, toxic ingredients. Using renewable feed stocks is one way to steer the plastic industry away from its

reliance on petroleum and create new pathways to the materials that are widely used today.<sup>3</sup>

Polyurethane foam is a plastic product used in insulation and cushioning across the packaging, automotive, construction, appliance, and footwear industries. This class of polymeric materials relies upon the reaction of polyols and isocyanates to form a polymer network within minutes, supporting a nascent cellular network that forms with the addition of a blowing agent. Isocyanates are a leading cause of workplace asthma, dangerous to manufacture, and hard to store.<sup>3,4</sup> Both respiratory and dermal exposure to isocyanates, even at low concentrations, have been shown to cause workplace asthma. Although the reported cases of workplace asthma have reduced due to increased use of proper PPE, it is still a cause for concern. The most common avenue for isocyanate exposure is spray foam slab stock polyurethane foam production.<sup>5,6</sup>

To address these concerns, non-isocyanate polyurethane (NIPU) foams have been a subject of research for about a decade. A polyurethane foam made without the use of isocyanates was first introduced by Cornille *et al.* in 2015.<sup>7</sup> Since then, many new formulas for NIPU foams can be found in the literature attempting to approximate the properties of the isocyanate-based foams currently on the market. Different

<sup>a</sup>Department of Food, Nutrition, and Packaging Science, Clemson University, Clemson, SC 29634, USA. E-mail: sternbe@clemson.edu

<sup>b</sup>US Department of Agriculture-Forest Service-Forest Products Laboratory, Madison, Wisconsin 53726, USA

<sup>c</sup>Center for Composite Materials, University of Delaware, Newark, DE-19716 2, USA. E-mail: spilla@udel.edu

<sup>d</sup>Department of Mechanical Engineering, University of Delaware, Newark, DE-19716, USA

<sup>e</sup>Department of Materials Science and Engineering, University of Delaware, Newark, DE-19716 8, USA

<sup>f</sup>Department of Chemical and Biomolecular Engineering, University of Delaware, Newark, DE-19716, USA



avenues to NIPU foams have been explored,<sup>8</sup> however, the majority of NIPU formulas use the route of polyaddition where a cyclocarbonate reacts with an amine to form the urethane structure without the release of a condensation product. Despite the success of this method, many formulas still use toxic ingredients such as epichlorohydrin and CO<sub>2</sub> insertion to create cyclocarbonate units<sup>9–12</sup> and other agents such as glutaraldehyde,<sup>13–15</sup> as well as hexamethylene diamine for curing.<sup>15–24</sup> Furthermore, many of the formulas present in the literature result in irregular cell structure, high densities, and rigid structures. Several non-isocyanate foams are reported in the literature, about half are rigid foams with densities ranging from 78–445 kg m<sup>−3</sup> (ref. 9, 13–15, 21, 22, 25–28) and the other half are flexible foams with densities ranging from 90–550 kg m<sup>−3</sup>.<sup>12,18,24,29–36</sup> Typically, the densities of commercial flexible polyurethane foams range from 10–80 kg m<sup>−3</sup> (ref. 37) and have compression strength values in the tens of kPa values.<sup>38</sup> The lightweight nature of flexible foams is important from the standpoint of applications such as seating, packaging, and automotive interiors.

Studies of flexible NIPU foams has struggled to reach the low-density nature of commercial flexible foams. Bourguignon *et al.* created self-blown NIPU foams from tri-carbonates with densities as low as 152 kg m<sup>−3</sup> and compression strengths of 50–1500 kPa.<sup>29</sup> Valette *et al.* used bio-based amino-telechelic oligomers and diamines to create NIPU foams with a siloxane as the blowing agent. The density reached as low as 130 kg m<sup>−3</sup> with compression strengths of 6–20 kPa.<sup>35</sup> Chen *et al.* created condensed tannin NIPU foams with densities as low as 150 kg m<sup>−3</sup> and compression strengths ranging from 288–500 kPa using a complex acid blowing agent.<sup>18</sup> The difficulty in matching typical PU foam properties lies in the ability to match the curing and blowing reaction of the foam. NIPU foams typically have slower curing times than the isocyanate-based process used in commercial formulations. External agents are often used in the blowing reaction with NIPUs, a more difficult process to control than the small addition of water (enabling the evolution of CO<sub>2</sub> gas) used in isocyanate-based reactions. These challenges have made it difficult to create NIPU foams below 100 kg m<sup>−3</sup> while maintaining the flexible nature of the materials. However, recent work has shown that faster, room temperature curing foam systems can be created with the addition of epoxy precursors, or others, to create internal heat for the foaming and curing reaction.<sup>39–41</sup> Using a combination of tricyclocarbonates and triglycidyl ethers, the work of Detrembleur and Grignard has resulted in foams with an internal density as low as 99 kg m<sup>−3</sup>.<sup>39</sup> Transitioning to glycerol-based (and thus biobased) cyclocarbonates and epoxies, the same group achieved similar physical properties with up to 90% biocontent.

Lignin is a naturally occurring phenolic polymer composing up to 35% of woody biomass.<sup>42</sup> A common commercial source of lignin is the kraft process where lignin is separated from cellulose fibers under alkaline conditions and high temperatures (170 °C).<sup>43</sup> Lignin contains abundant reactive hydroxyl groups, valuable for polyurethane chemistry. However, its crosslinked structure results in low solubility and reactivity,

making it susceptible to unwanted side reactions that complicate processing and reduce efficiency. Because of these challenges, lignin-based PUs have not found commercial adoption whether using isocyanates or not. Most efforts toward lignin-based PU foams continue to rely on isocyanates and only reach 10–20% lignin content before drastically increasing density or falling short of the required properties.<sup>44,45</sup> Lignin-based NIPU foams are more rare and reaching the properties similar to other NIPU foams, or those of commercial interest, is still an active research area. Lignin as a filler has been added to NIPU formulations to utilize water trapped in its own polymer matrix to assist with foaming,<sup>46</sup> however, the density of the lignin-based foams was much higher than traditional flexible PU foams (222–319 kg m<sup>−3</sup>). In addition, lignin has been explored as a source of cyclocarbonate for flexible NIPU foams used in wound dressing,<sup>47</sup> however, a full physical and chemical characterization of the foams was not completed as the main purpose of the study was directed at antimicrobial properties of the dressings. In our first report, we demonstrated that high density, rigid NIPU foams could be synthesized from cyclocarbonated kraft lignin and a dimer diamine.<sup>25</sup> However, reaching the low-density and flexible nature of typical commercial PU foams was not achieved.

To address the current limitations associated with lignin-based NIPU foams, our research focuses on creating a reaction system using lignin, and another castor-oil based reagent, to align the curing and blowing reaction to create foams with densities below 100 kg m<sup>−3</sup>. The uniqueness of our approach is the use of lignin in high concentrations as a biobased cross-linker, as well as other biobased sources from castor oil and fatty acids, to enable a nearly 100% biobased formulation. Poly(methylhydrosiloxane) was used for chemical foaming due to its ability to react with diamines and evolve hydrogen gas. This study exists as a demonstration of how lignin can be used in high concentrations toward a commodity polymer application, and explores the structure–property relationships of different reaction mixture formulations.

## Materials and methods

### Materials

Kraft lignin for this study was supplied by the Ingevity Corporation (North Charleston, SC, USA) under the trade name “Indulin® AT”. Indulin® AT is a softwood kraft lignin<sup>48</sup> and was dried under vacuum at 30 °C overnight before use. The hydroxyl content and molecular weight of the as-received kraft lignin can be found in Table SII. The curing agent was kindly provided by Cargill under the trade name “Priamine™ 1074”. Priamine™ is a dimer diamine with an amine value of 209 mg KOH per g.<sup>25</sup> The silicone based surfactant was kindly provided by the Evonik Corporation (Hopewell, VA, USA) under the trade name TEGOSTAB® B 8993. The catalyst, 1,5,7-triazabicyclo[4.4.0]dec-5-ene (>98.0%) (TBD), was purchased from Tokyo Chemical Industry (Tokyo, Japan). Dimethyl carbonate (99%) (DMC), and sebacoyl chloride (97%) were purchased from BeanTown Chemical (Hudson, NH, USA). Glycerol, dimethylsulfoxide (DMSO), potassium carbonate, and triethylamine (TEA) were



purchased from VWR (BDH) Chemicals LLC (Randor, PA, USA). Dichloromethane ( $\geq 99.5\%$ ) (DCM), poly(methylhydrosiloxane) (PMHS), 1,3,5-trioxane ( $>99\%$ ), chromium(III) acetylacetonate, 2-chloro-4,4,5,5-tetramethyl-1,3,2-dioxaphospholane (95%), cholesterol, chloroform-d<sub>1</sub>, and dimethylsulfoxide-d<sub>6</sub> (DMSO-d<sub>6</sub>) were purchased from Millipore Sigma (St Louis, MO, USA). Pyridine was purchased from Avantor Performance Materials LLC (Randor, PA, USA). The polyol and diisocyanate were kindly provided by Huntsman Chemical (The Woodlands, TX, USA).

The following set of chemicals were used to make the large scale CC lignin. Glycerine (USP Grade) was purchased from Colonial Chemical Solutions (Savannah, GA). Dimethyl sulfoxide was purchased from Oakwood Chemical (Estill, SC). Dimethyl carbonate was purchased from Shandong Greenfood Import Export Co. (Xintai, Shangdong Province, China). Potassium carbonate (anhydrous) was purchased from Thermo Fisher Scientific (Ward Hill, MA).

### Glycerol carbonate

Glycerol carbonate (GC) was synthesized according to a previous report.<sup>49</sup> Briefly, glycerol, previously dried by distillation under vacuum, was mixed in a round bottom flask with 3 equivalents dimethyl carbonate (DMC). The catalyst, potassium carbonate, was added in 0.1 equivalents and the reaction was conducted at 73 °C for 1.5 h. When the reaction was completed, the methanol generated and excess DMC were removed under reduced pressure. Yields were quantitative.

<sup>13</sup>C NMR (75 MHz, C<sub>2</sub>H<sub>6</sub>OS,  $\delta$ , ppm): 155.6 (s, Cd), 77.4 (s, Cb), 66.3 (s, Cc), 61.0 (s, Ca) (Fig. S1).

### Lignin functionalization

**Large scale cyclocarbonated lignin.** Lignin, 2 kg dried under vacuum at 30 °C (11.28 mol OH), was mixed with 10 L of glycerol carbonate (118.6 mol) reagent, utilizing the residual potassium carbonate catalysts from GC synthesis (0.1 equivalents), in a 20 L stainless steel Parr reactor equipped with impellers and an anchor stirrer. The reactor was flushed with nitrogen and heated to 145 °C and held at temperature for 45 minutes. The carbon dioxide generated produced a final pressure of 2.3 MPa. The reactor was reduced from the heating mantle and allowed to cool overnight with stirring while slowly releasing the carbon dioxide pressure. Then, the functionalized lignin was slowly pumped into 180 L water and gently mixed for 30 minutes before the pH was reduced to 3 using sulfuric acid. The functionalized lignin was allowed to settle overnight and about 120 L of supernatant decanted from the settled lignin. The lignin was twice washed by being resuspended into 900 L of pH 3 water, allowed to settle, followed by decanting about 850 L of supernatant. The functionalized lignin was filtered, air-dried and then dried under vacuum at 30 °C. The functionalized lignin, 2.1 kg, was mixed with 400 g potassium carbonate, 4 L dimethyl sulfoxide and 6 L dimethyl carbonate in a 20 L stainless steel Parr reactor and mixed at room temperature for 2 hours under a nitrogen atmosphere. The reactor was heated to 75 °C for 2 hours, then cooled to room temperature with a water bath. The cyclocarbonated lignin (CC lignin) was precipitated by

transferring into 180 L of water adjusted to pH 3 with sulfuric acid and mixed for 30 minutes. The cyclocarbonated lignin was allowed to settle overnight and about 120 L of supernatant decanted from the settled lignin. The lignin was twice washed by being resuspended into 900 L of pH 3 water, allowed to settle followed by decanting about 850 L of supernatant. The functionalized lignin was filtered, air-dried and then dried under vacuum at 30 °C yielding 2.05 kg of cyclocarbonated lignin.

**Laboratory scale cyclocarbonated lignin.** Laboratory batches of cyclocarbonated lignin were completed according to our previous report.<sup>25</sup> Briefly, 10 grams of lignin was mixed with 50 mL of GC containing residual potassium carbonate catalyst from GC synthesis (0.1 equivalents) ensuring a greater-than 10 $\times$  equivalent of GC : hydroxyl groups of lignin, with enough liquid volume to fully dissolve lignin (56.4 mmol OH : 593 mmol GC). The reactants were heated slowly to 150 °C for a total reaction time of 1.5 h. Once cooled, the oxyalkylated product was precipitated with acidified water, filtered, and washed with deionized water. After drying overnight under vacuum, typical yields of the oxyalkylated lignin resulted in a mass increase of 23% based on initial lignin mass. Cyclocarbonated lignin (CC lignin) was produced through a ring closing reaction with 5 equivalents of DMC (according to the OH content of oxyalkylated lignin) for 2–6 hours. Typical yields were 94% of the starting mass of oxyalkylated lignin. To determine the optimal time for the ring closing reaction, samples were removed at 2, 4, and 6 hours. <sup>13</sup>C NMR analysis was performed on each sample and the cyclocarbonate concentration was determined using trioxane as an internal standard (Table SII). The resulting NMR spectrum for the 6 hour sample is shown in Fig. S2.

### Sebacic bicyclic carbonate

Sebacic bicyclic carbonate (SebCC) was synthesized according to Carré *et al.*<sup>50</sup> DCM, and TEA (1.1 equivalents) were added to a round bottom flask with a 3-fold excess of GC. Sebacyl chloride (1 equivalent) was added dropwise to the round bottom flask. The reaction was conducted overnight in an ice bath under nitrogen. When the reaction was completed, the precipitate was removed by vacuum filtration and the liquid phase was retained after washing the solids with several aliquots of DCM. The product was then washed with 5 wt% hydrochloric acid solution to remove excess GC, dried with magnesium sulfate, and the solvent was evaporated to leave a crystalline white solid. Typical yields were 63  $\pm$  9.6%.

<sup>13</sup>C NMR (75 MHz, DMSO-d<sub>6</sub>,  $\delta$ , ppm): 173.0 (s, Cd), 155.1 (s, Ch), 74.7 (s, Cf), 66.4 (s, Ce), 63.5 (s, Cg), 33.6 (s, Cb), 28.8 (d,  $J$  = 11.2 Hz, Ca), and 24.7 (s, Cc) (Fig. S6).

### NIPU foam

NIPU foams were synthesized from large scale CC lignin synthesis by dissolving CC lignin, catalyst, surfactant and SebCC at a ratio of 1.3 mL DMSO : 1 g CC lignin in an aluminum mold using an internal temperature of 70–80 °C. Table 1 displays the amounts and molar ratios of the components described here. The dimer diamine was then added and the mixture was allowed to react for 4–5 minutes to increase the



**Table 1** Compositions of NIPU foams using multiple SebCC to CC lignin ratios. CC : amine ratios were calculated by first subtracting the consumption of amine by the blowing agent, PMHS, assuming 90 wt% hydrosiloxane unit. Catalyst: TBD, surfactant: TEGOSTAB® B 8993

Sample	NIPU A	NIPU B	NIPU C
CC lignin (g, mmol CC)	2.00, 3.2	2.00, 3.2	1.00, 1.6
SebCC (g, mmol CC)	1.00, 5.0	2.00, 10.0	2.00, 10.0
Catalyst (g)	0.06	0.19	0.17
Surfactant (μL)	160	360	308
Blowing agent (μL)	150	150	100
Amine (mL, mmol NH <sub>2</sub> )	2.50, 8.4	3.00, 12.2	2.40, 8.0
CC : amine	1.3	1.7	1.8

viscosity before foaming. Then, the foaming agent, PMHS, was added and stirred manually before placing in an oven set at 150 °C for 4–6 hours. The foaming agent reacts with the diamine present in the formulation to release hydrogen gas and was added between 2–3 wt% similar to our earlier report.<sup>25</sup> The amount of amine consumed by the foaming agent was calculated by taking the hydrosiloxane unit as 90 wt% composition of PMHS.<sup>7</sup> The resulting amount of amine groups were compared to CC groups and presented in Table 1. Once cured, the foams were removed from the mold and either used in their cylindrical form or cut into cubes for further analyses.

### Flexible PU foam reference

The flexible polyurethane reference foam was synthesized using the one-shot method where polyol and diisocyanate (polymeric diphenylmethane diisocyanate, pMDI) were mixed in an open cup and allowed to cure at ambient conditions. The polyol had a hydroxyl number of 163.2 mg KOH and the pMDI was 29.8% NCO. The pMDI and polyol were added with an isocyanate index of 100 and stirred manually until foaming began. The final foam samples were cut into cubes for further analysis.

### Characterization

**Density calculation.** The apparent density of foams was determined by cutting each sample into a cylindrical shape of approximately 40 mm diameter, and measuring the diameter and height three times to obtain an average volume for each cut sample. All densities were determined as an average of four samples.

**Scanning electron microscopy.** Scanning electron microscopy (SEM) was completed using a Hitachi 3400. The samples were cut to dimensions of 1 × 1.5 × 0.5 mm and sputtered with platinum. The electron beam was operated at a voltage setting of 10 kV. The average cell lengths were determined by measuring the lengths of approximately ten cells in the SEM image using ImageJ software.

**Gel content.** Gel content was measured by placing 30 g of NIPU foam in 30 mL of DMSO and soaking for 24 hours. After soaking, the samples were removed and dried under vacuum at 70 °C for 24 hours. Once dried, the samples were weighed, and gel content was calculated using eqn (1)

$$GC\% = \frac{\text{Dry weight}}{\text{Initial weight}} \times 100 \quad (1)$$

**Compression force deflection.** Compression testing was performed on an Instron 6800 using a 2580 series load cell (500 N) and a 2501 series compression platens. Compression force deflection was determined according to ASTM D3574 (ref. 51) with some modifications using an average of four samples. An initial cyclic compression to 20% was applied at a rate of 250 ± 5 mm min<sup>−1</sup> for two cycles. The sample was then allowed to rest for 60 seconds before compressing the foam to 50% at a rate of 50 ± 5 mm min<sup>−1</sup>. The force at 50% was recorded at time 0 and held at 50% compression for 60 seconds where the final value was recorded. The specific compression force deflection value was found by dividing the compression force deflection value at 60 seconds by the respective density of each foam.

**Differential scanning calorimetry.** All differential scanning calorimetry (DSC) tests were run using the TA Instruments Discovery DSC 250. DSC was performed using 2–4 mg samples and a heat–cool–heat cycle between −50 and 200 °C at a heating rate of 10 °C per minute. The glass transition temperature was determined from the second heating cycle.

**Thermogravimetric analysis.** All TGA tests were run using a TA Instruments AutoTGA 2950 V5.4A. Samples of 3–10 mg were heated under nitrogen from room temperature to 700 °C with a heating rate 10 °C per minute.

**Burn testing.** Burn testing was conducted following ASTM D4986,<sup>52</sup> with some modifications in sample size. All samples were cut into rectangular shapes measuring 25 × 22 × 13 mm, and the tops of the samples were marked at 4, 10, and 21 mm. Samples were placed on a wire grate and ignited on one end by a wing-top burner fueled by natural gas. The time the flame reached each mark and the total burn time were recorded. A cotton indicator was placed below the sample to record ignition from falling debris.

**Fourier transform infrared spectroscopy.** Fourier transform infrared spectroscopy (FTIR) was run using a Thermo Fisher Nicolet™ iS™ 10 ATR Spectrometer from 400–4000 cm<sup>−1</sup> using 16 scans with 2 cm<sup>−1</sup> spectral resolution.

**Nuclear magnetic resonance.** Nuclear magnetic resonance (NMR) analysis was performed using a Bruker Avance 300 MHz spectrometer. <sup>13</sup>C NMR was performed on CC lignin samples to determine cyclocarbonate concentration by dissolving 100 mg of sample and 50 mg trioxane, as an internal standard, in 1 mL DMSO-d<sub>6</sub>. Chromium(III) acetylacetonate was used as a relaxation agent with a spectral window of 18 110 Hz and 20 000 scans. For SebCC samples, 200 mg of sample and 100 mg trioxane were dissolved in 1 mL DMSO-d<sub>6</sub> and run for 100 scans. For GC samples, 50 mg of sample was dissolved in 1 mL DMSO-d<sub>6</sub> and run for 100 scans. <sup>31</sup>P NMR analysis was run on kraft lignin samples to determine hydroxyl content. <sup>31</sup>P NMR was run according to previously described methodology using 2-chloro-4,4,5,5-tetramethyl-1,3,2-dioxaphospholane as a phosphorolating agent in a 1.6/1 solution of pyridine and chloroform d-1.<sup>53</sup> Cholesterol was used as an internal standard and chromium(III) acetylacetonate as a relaxation agent. 2D HSQC spectra of kraft





lignin and the masterbatch of cyclocarbonated lignin were collected on a Bruker Avance 500 MHz spectrometer equipped with a BBO probe, using the standard Bruker pulse sequence hsqcetgppsp.3 (phase-sensitive, gradient-edited 2D HSQC employing adiabatic pulses for inversion and refocusing). A total of 2000 data points were collected over a 12 ppm spectral width in the F2 ( $^1\text{H}$ ) dimension with an acquisition time of 170 ms. For the F1 ( $^{13}\text{C}$ ) dimension, a spectral width of 40 ppm and an acquisition time of 6.36 ms were employed.

**Gel permeation chromatography.** Gel permeation chromatography (GPC) was performed using multi-angle static light scattering (MALS) on the DAWN from WYATT technology for GPC data presented in Table SI. Measurements were performed according to the procedure outlined by Tindall *et al.*<sup>54</sup> In short, separation was performed using Styragel HT5 and Agilent PolarGel-L columns in series. Lignin was dissolved in HPLC-grade *N,N*-dimethylformamide with 0.05 M lithium bromide. The mobile phase was filtered with a 0.20  $\mu\text{m}$  PTFE syringe filter at a flow rate of 0.6  $\text{mL min}^{-1}$ .

For GPC data in Table SII, GPC measurements were performed using an EcoSEC Elite® GPC System with RI detector and four columns in series: one TSKgel SuperAW-L guard column, two TSKgel SuperAWM-H columns, and one TSKgel SuperAW2500 column. Samples were dissolved in dimethylacetamide with 0.05 wt% lithium bromide. The flow rate of the mobile phase was 0.4  $\text{mL min}^{-1}$  with an injection volume of 80  $\mu\text{L}$ .

**Rheometry.** Reaction mixture viscosity was measured using a TA Instruments Discovery HR-2 Rheometer using 25 mm parallel plates. Reaction mixtures in Table 1 were mixed without foaming agent and then placed on the plates set to a gap width of 1 mm. The initial viscosity building stage used in the synthetic technique described above (4–5 minutes at 70  $^\circ\text{C}$ ) was replicated by allowing the reaction mixture to soak on the plates at 70  $^\circ\text{C}$  for four minutes. Next, the temperature was increased at 10  $^\circ\text{C min}^{-1}$  under 1% strain and 10  $\text{rad s}^{-1}$  until 150  $^\circ\text{C}$ . Complex viscosity was read as steady shear viscosity according to the Cox–Merz rule.<sup>55</sup>

## Results and discussion

### Cyclocarbonated lignin synthesis

In this study, a 2 kg batch of CC lignin was produced for foam synthesis to minimize batch-to-batch variability and demonstrate the ability to move beyond small-scale laboratory synthesis. The larger synthesis was completed in a 20 L Parr reactor compared to glassware on the order of 1 L used in laboratory trials. Due to the tendency of the reaction mixture of glycerol carbonate and kraft lignin to foam during the initial temperature ramp to 145  $^\circ\text{C}$ , scale-up reactions used a closed vessel due to limited head-space and monitored the pressure inside the vessel for the extent of reaction. The temperature of the Parr reactor was increased slowly and maintained at 145  $^\circ\text{C}$  for a total reaction time of 1.5 h. In the second step, a ring-closing transesterification reaction using dimethyl carbonate was completed in the same Parr reactor after washing and drying of the oxyalkylated kraft lignin. Laboratory trials were

used to determine a favorable reaction time (2 h) that enabled cyclocarbonate conversion and limited crosslinking reactions that would increase molecular weight (Table SII). The  $^{13}\text{C}$  NMR spectrum showed the characteristic peaks for oxygenated units corresponding to the cyclocarbonate rings (Fig. S3) along with a sharp peak at 155 ppm corresponding to the carbonyl group of the cyclocarbonate. 2D NMR of kraft lignin before (Fig. S4) and after (Fig. S5) cyclocarbonation shows a decrease in the signal associated with gamma hydroxyls in the  $\beta$ -O-4 interunit links, as well as new regions of intensity corresponding to cyclocarbonate rings. The larger-scale synthesis resulted in a slightly lower CC content compared to laboratory trials (*cf.* 1.6 vs. 2.2  $\text{mmol g}^{-1}$  in Table SII). The larger batch of CC lignin demonstrated very similar  $M_w$  values but lower  $M_n$  values leading to a higher polydispersity compared to laboratory trials (Table SII). Controlling the molecular weight of CC lignin after functionalization was found to be key to successful foam synthesis (see below), however, the foam properties demonstrated here show the successful scale-up of the organic carbonate-pathway to lignin-based cyclocarbonates at the kilogram scale.

### Synthesis and design of NIPU foam

The use of lignin in a foam structure presents the challenges of lignin's low solubility, reactivity, and crosslinked nature often leading to irregular cell morphology and unreacted material when used in typical PU formulations.<sup>44,56</sup> Similar challenges exist for employing lignin in a NIPU foam, especially since successful foams are still based on timing the gelling and foaming reaction to prevent cellular collapse and to create low-density materials. In our past work, we found that CC lignin, dissolved in a small amount of DMSO, gelled quickly enough with a dimer diamine curing agent (DDA, Fig. 2) to enable foaming with PMHS.<sup>25</sup> However, this 2-component mixture did not allow an extensive rise of the foam and led to high density,

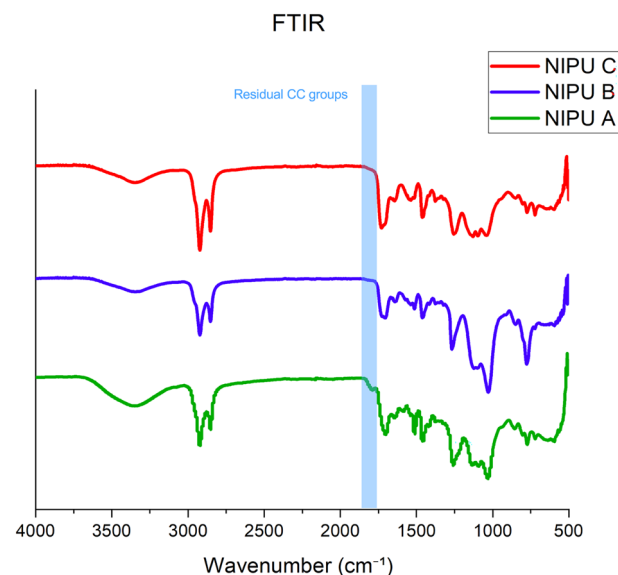


Fig. 1 FTIR of NIPU foams.



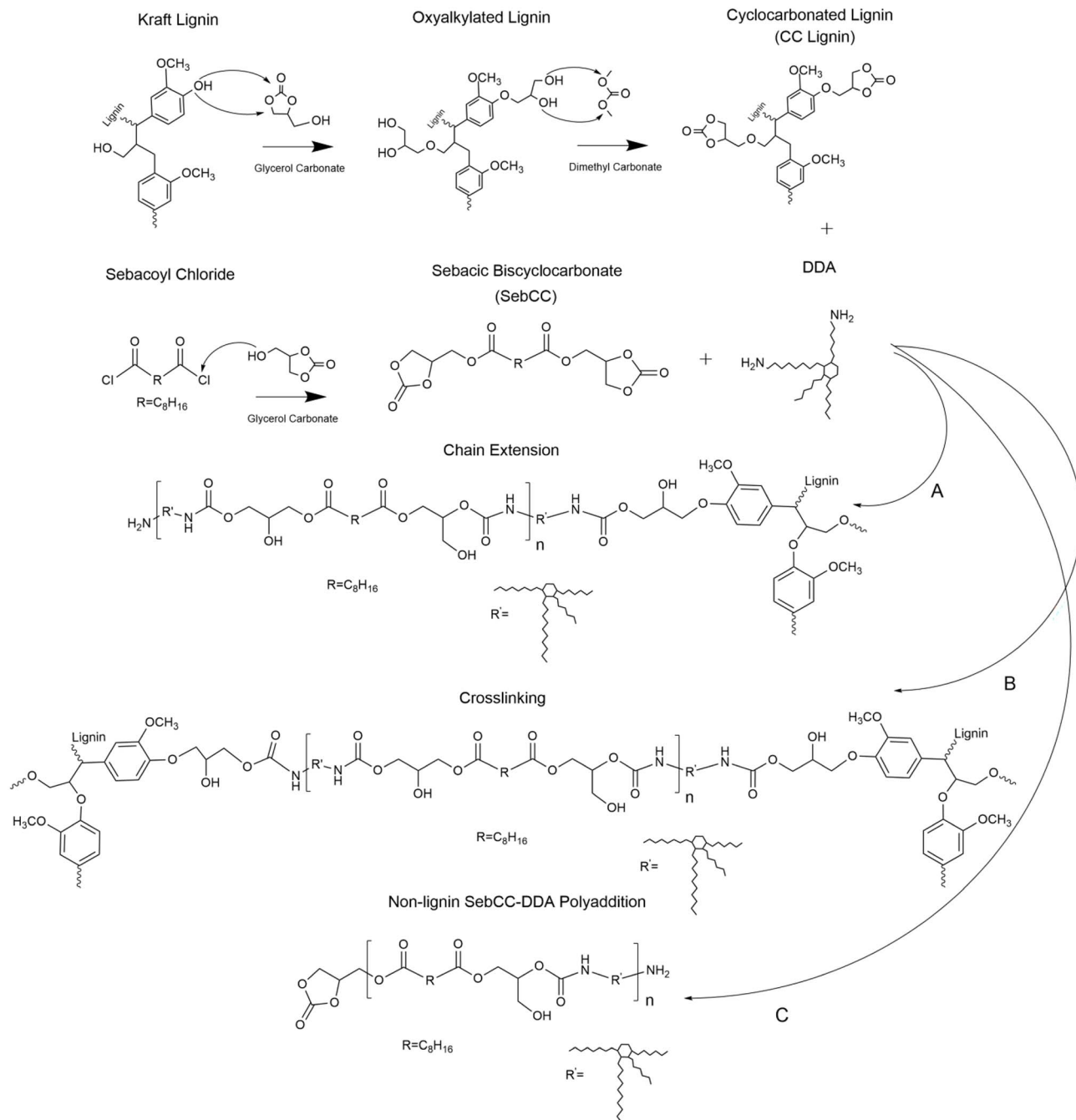


Fig. 2 NIPU reaction scheme.

rigid foams ( $\rho = 240 \text{ kg m}^{-3}$ ). Given lignin's high molecular weight and crosslinked nature, we sought the addition of a more flexible, aliphatic component that might mimic the low viscosity nature of polyether polyols used in traditional, flexible PU foams. Aligning with the 100% biobased nature of our previous formulation, sebacic bicyclic carbonate (SebCC), derived from castor oil, was identified in the literature as a potential chain extender and rheology modifier given previous reports on its successful use in thermoplastic NIPU polymer synthesis.<sup>50,57</sup> A traditional isocyanate-based flexible foam was

also synthesized as a basis of comparison against the new lignin-derived formulations.

SebCC is a low melting point ( $\sim 70^\circ\text{C}$ ) solid at room temperature and can be synthesized from either sebacic acid, or sebacoyl chloride, both castor oil derivatives. Reaction mixtures (Table 1) were composed of 2 : 1 ("NIPU A"), 1 : 1 ("NIPU B") and 1 : 2 ("NIPU C") weight ratios of CC lignin : SebCC that were mixed together in an aluminum mold at  $70\text{--}80^\circ\text{C}$  before the surfactant, catalyst and curing agent were added and allowed to build viscosity for 4–5 minutes. Then, the foaming agent, PMHS, was added and stirred manually before being placed in

an oven at 150 °C. Initially, stoichiometric amounts of CC units, amine, and foaming agent were used to synthesized foams. However, foam collapse was observed at this stoichiometry along with the observation of a sticky residue present. The diamine amount was then decreased to sub-stoichiometric amounts (Table 1) and positive results were obtained. While stoichiometric equivalencies of amine and CC are normally required for linear polyaddition reactions, the crosslinked system employed here (Fig. 2) has many crosslinking points per lignin unit and different reactions that could take place. Indeed, the chain extension and non-lignin polyaddition reaction between SebCC and the aliphatic diamine (Fig. 2A and C) would occur side-by-side with crosslinking reactions (Fig. 2B). While crosslinking reactions would build reaction mixture viscosity and hasten the point to gelling, extension reactions, or reactions not involving lignin at all, would most likely lower the viscosity due to the increased molecular motion of flexible, aliphatic chains in the polymer matrix and polymer softening at the elevated temperatures during curing. Previous studies using SebCC and the same dimer diamine employed here demonstrated amorphous, thermoplastic properties with increased polymer flow above room temperature.<sup>50</sup> Lowering the amount of dimer diamine allowed the reaction mixture to reach a gel-point in sufficient time to enable the cellular morphology to develop, while not softening or collapsing as the matrix heated-up to the curing temperature of 150 °C. Further exploration of the effect of SebCC on the reaction mixture viscosity is evaluated below using rheometry.

The extent of the reaction between CC units and amines was monitored by following the conversion of the CC FTIR signal at 1800 cm<sup>-1</sup> to that of the urethane signal at ~1720 cm<sup>-1</sup>. Fig. 1 shows that for all formulations, a nearly full conversion of CC units is observed. While the diamine was added in sub-stoichiometric amounts that should result in unreacted CC groups, CC units could also react with residual water present in lignin or the solvent used for dissolving the components, DMSO, especially since the foams were synthesized in open-air conditions where moisture could have been absorbed. Given the stoichiometry used to synthesize the foams, as little as 1 microliter (5.5 mmol) of water would be enough to consume the residual CC units in the reaction mixture formulations.

The inclusion of a surfactant and SebCC led to an immense improvement in the foaming ability and rise height of the lignin-based foams compared to our previous studies.<sup>25</sup> NIPU "A" and "B" both demonstrated average densities below 100 kg m<sup>-3</sup> with compression strength values typical for flexible foams. As with conventional isocyanate PU foams, the foam structure was highly dependent upon the surfactant used during synthesis. Given the proprietary nature of commercial surfactants and the limited amount of structural information that is available, a screening approach was taken to identify the best performing surfactant among a series of products advertised for PU foams. Several surfactants were tried in the 8000 series of Evonik's Tegostab® products. The best performing surfactant was identified as 8993, advertised as a strong cell regulator for footwear applications. Given the challenges associated with regulating cell size and shape associated with lignin-based

foams, the cell regulating properties of this surfactant were found to be very beneficial.

Rheological experiments were conducted without the use of a foaming agent to measure the rise in viscosity during the first several minutes of curing to understand the influence of SebCC on the improved ability to create low-density foams. Typical PU foams make use of polyols with initial viscosities in the tens of Pa s that lead to the gel point of the mixture at which the cellular structure is set through sufficient network formation and/or entanglement.<sup>58</sup> The formulations used to prepare NIPU A and B display viscosity values in this range at temperatures between 100–120 °C (Fig. 3), 1–2 orders of magnitude lower than when CC lignin alone was used as precursor mirroring our previous report<sup>25</sup> (Fig. 3). Thus, the addition of SebCC lowers the viscosity of the nascent reaction mixture, creating more favorable conditions for foaming while also reacting fast enough to prevent cellular collapse. The gel point is another important parameter as cellular collapse will occur if the expanded reaction mixture is not set in a short amount of time. The gel point is often determined from the crossover of storage and loss modulus, the point where the mixture takes on solid-like properties, rather than being dominated by a viscous response. While all formulations reach this point between 100–120 °C (Fig. S5), it is important to note the viscosity of each formulation during this temperature regime. The formulations that resulted in the lowest densities, NIPU A and B, display complex viscosity in typical PU ranges (*i.e.* 5–20 Pa s) while NIPU C has a much lower viscosity until it reaches approximately 140 °C (Fig. 3). This delay in reaching an adequate viscosity value results in the release of foaming agent without expansion, creating a higher density material (Table 2,  $\rho = 268 \text{ kg m}^{-3}$ ). Formulations for NIPU A and B thus demonstrate reaction kinetics and viscosity conducive to timing the foaming and

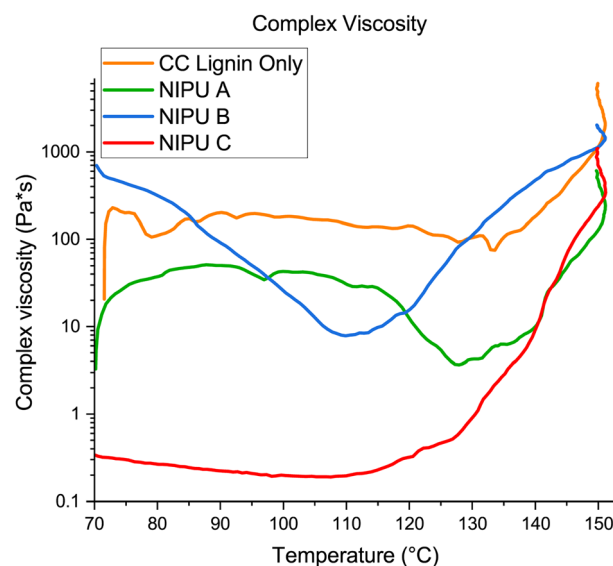


Fig. 3 Complex viscosity of NIPU formulations A–C without foaming agent compared to a previous formulation without SebCC or surfactant<sup>25</sup> (CC lignin only).



**Table 2** Characteristics of NIPU foams using multiple SebCC to CC lignin ratios. GC: gel content,  $\rho$ : density, cell size: average cell diameter, CF: compression strength at 50% compression, CFD at 60 s: compression force deflection at 50% compression after 60 seconds, SCFD at 60 s: compression force deflection normalized for density

Sample	$\rho$ (kg m <sup>-3</sup> )	Cell size (mm)	GC (%)	CF (kPa)	CFD at 60 s (kPa)	SCFD at 60 s (kPa/ $\rho$ )
NIPU A	95.96 $\pm$ 5.75	1.23 $\pm$ 0.29	86	25.1 $\pm$ 5.2	13.1 $\pm$ 2.7	0.14
NIPU B	98.44 $\pm$ 13.22	1.01 $\pm$ 0.38	73	14.8 $\pm$ 1.5	6.3 $\pm$ 0.5	0.06
NIPU C	268.11 $\pm$ 110.60	1.52 $\pm$ 0.52	63	29.8 $\pm$ 15.6	11.4 $\pm$ 5.7	0.04
PU ref	60.35 $\pm$ 4.95	0.55 $\pm$ 0.09	N/A	9.9 $\pm$ 0.2	7.6 $\pm$ 0.2	0.13

curing reactions, necessary for reaching the goal of low-density foams below 100 kg m<sup>-3</sup>.

### Physical and mechanical properties

Flexible polyurethane foams are typically characterized by open cells. However, Fig. 5 indicates the presence of some closed cells in the lignin-based NIPUs, most likely resulting from the crosslinking provided by CC lignin. Lignin represents a large proportion of the foam formulation, ranging from 35.6% in NIPU A down to 17.4% in NIPU C. A general increase in open cells can be observed with an increase in SebCC concentration as crosslinking would decrease due SebCC's bifunctional, linear nature. This hypothesis is supported by gel content analysis, where NIPU A had a 86% gel content, but that of NIPU B and C decreased to 73% and 63%, respectively (Table 2). Compared to our previously studied rigid foams, the overall cell sizes in the samples studied here are smaller. Cell sizes for the previously reported rigid foams were approximately 2 mm and the cells for NIPU A to C range between 1.0 and 1.5 mm.<sup>25</sup> However, compared to the cellular structure of the polyurethane standard, the NIPU foams are larger and more irregular. Smaller, homogeneous cells are typically considered more desirable for most applications.

While rigid foams typically have compression force deflection values above 100 kPa for 10% compression, flexible foams demonstrate values in the tens of kPa at 50% compression, which is the strain value typically used for testing.<sup>38</sup> NIPUs A–C demonstrate flexible behavior with compression force deflection values between 15–30 kPa, slightly higher than the PU reference (Table 2). Compression force deflection (CFD) uses a pre-strain cyclic mode, followed by compression to 50% strain, then a holding period where the final compression value is recorded after 60 seconds. This test measures the ability of a material to respond to constant stress. NIPU A demonstrates a higher CFD than NIPU B, corresponding to the higher lignin ratio present in its formulation. NIPU C, containing the lowest amount of lignin, has the highest CFD, although this is explained by its density, which is almost 3 times as high as NIPU A and B. Lignin improves the fatigue response by maintaining more of the initial stress response after 60 seconds. For example, the CFD of NIPU A at 60 s is 52.2% of its initial compressive stress value while NIPU B and C's CFD values are 42.5% and 28.2%, respectively. The greater crosslinking afforded by lignin minimizes the collapse of cells under constant stress, leading to lower fatigue of the material. The higher

closed-cell content of NIPU A, compared to the increasing open-cell content of NIPU B and C, also contributes to a lower fatigue response as closed cells provide greater structural support than open cells. The specific CFD value, where density is used to normalize the result, decreases from NIPU A to C as the lignin content decreases and the more flexible, aliphatic SebCC content increases. Examining the stress–strain behavior of the foams (Fig. 4), most of the compression observed lies within a plateau region, which corresponds to the collapse of the cells resulting from compression.<sup>59</sup> The trend of a large plateau region is typical in compression testing for isocyanate-based flexible polyurethane foams up to 50% compression.<sup>60</sup> The lack of a clear linear elastic region is most likely due to the irregular cell structure of the lignin NIPUs, as the PU reference demonstrated a more pronounced linear region of compression (Fig. 4). Slight densification regions are observed for low density materials NIPU A and B, however, for NIPU C there is a more pronounced densification region referring to the complete compression of cells walls.

The success of foam synthesis was found to be highly dependent upon the CC lignin precursor used in foam formulations. Laboratory studies were conducted to understand the influence of the reaction parameters leading to CC lignin and

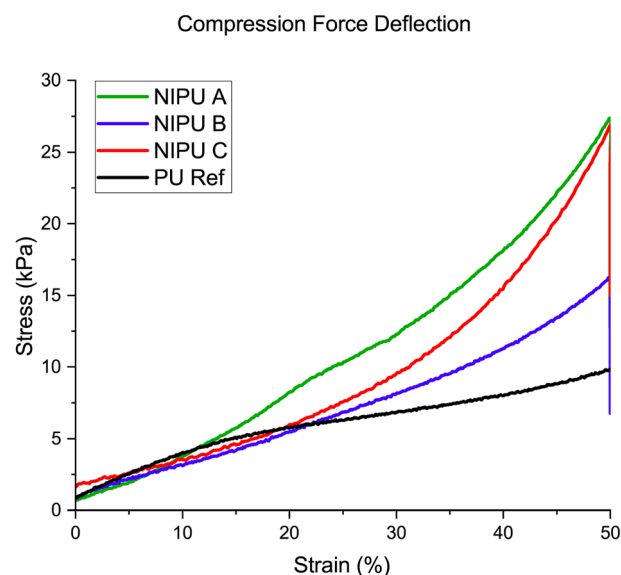


**Fig. 4** Compression force deflection curves of NIPU foams with different ratios of SebCC to CC lignin and PU ref.





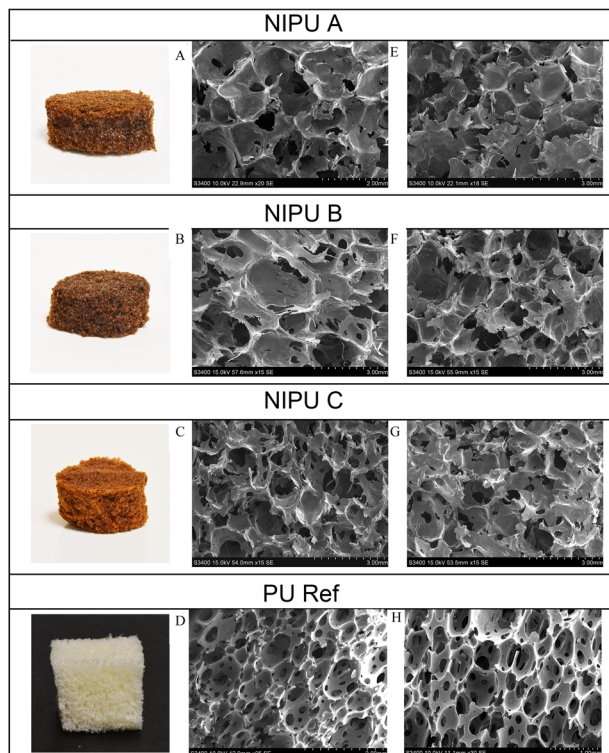


Fig. 5 SEM of NIPU foams of the three different formulas. (A–C) Side of NIPU foam, (E–G) top of NIPU foam, (D) and (H) varying magnifications of the reference isocyanate based PU foam.

understand their effect on foam synthesis. The synthetic pathway leading to CC lignin was prone to side reactions where a large increase in reaction mixture viscosity and gas release was observed in oxyalkylation, and agglomeration of the product was often observed in ring closing by DMC. These side reactions were often hard to control, occurring with slight differences in temperature ramp, reaction time, or moisture content. The

molecular weight of lignin was observed to increase with reaction time during the ring closing reaction with DMC. The molecular weight increased from 37.2 kDa to 58.0 kDa at a reaction time from 2 to 6 hours, while the polydispersity value increased from 6.0 to 9.2 (Table SII). These studies were used to inform the reaction time (2 h) for the large scale synthesis. Molecular weight increase most likely results from crosslinking reactions at linear carbonate sites formed during the oxyalkylation reaction or crosslinking with DMC through the residual hydroxyl groups on lignin. Several groups have observed similar reactions and molecular weight increases during the reaction of lignin with organic carbonates.<sup>61–64</sup> It was observed over the course of experiments that collapsed foams often came from CC lignin of much higher molecular weight,

Table 3 Table of thermal properties.  $T_g$ : glass transition temperature,  $T_d5\%$ : temperature of 5% thermal decomposition

Sample	$T_g$ (°C)	$T_d5\%$ (°C)	Char yield (%)
NIPU A	−14.98	197.55	16.83
NIPU B	−18.34	219.76	16.70
NIPU C	−18.33	247.72	12.56
PU ref	36.21	277.90	7.62



Fig. 7 Remnants of NIPU foam samples after burn testing.

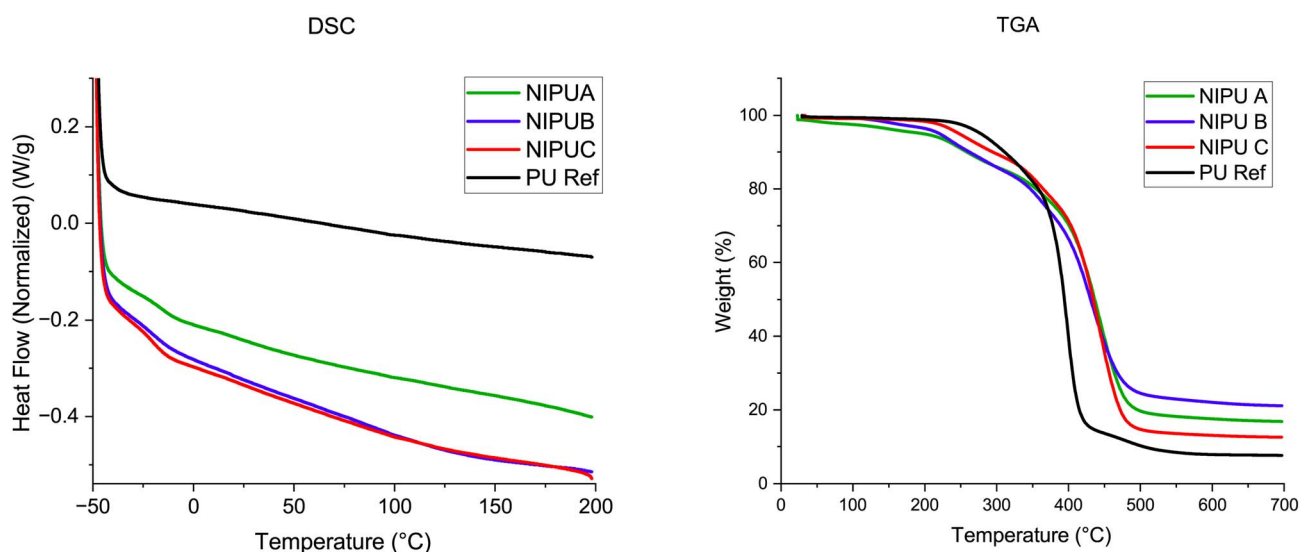


Fig. 6 DSC and TGA of the three NIPU foams and PU ref.



**Table 4** Table of burn testing results. Afterburn: timelength of visible flame after removing heat source

Sample	Burn rate (mm s <sup>-1</sup> )	Afterburn (s)	Cotton drip ignition	Complete combustion
NIPU A	0.79 ± 0.23	89.31 ± 20.37	No	No
NIPU B	0.86 ± 0.26	81.54 ± 11.93	No	No
NIPU C	0.59 ± 0.56	58.85 ± 63.07	No	No
PU ref	1.22 ± 0.11	31.2 ± 3.77	Yes	Yes

whereas foams with good morphology and curing characteristics came from CC lignin where the molecular weight was lower (see Table SI). Controlling the reaction sequence towards CC lignin was a key parameter to enable low-density, flexible materials.

### Thermal properties

Thermal properties of the NIPU foams were analyzed using DSC and TGA and compared to the results of the PU reference sample. DSC traces exhibited no endotherms associated with melting, consistent with the crosslinked nature of the foam material. All formulations showed a glass transition temperature ( $T_g$ ), located by the change in slope of the second heating curve (Fig. 6), below 0 °C, lower than the PU reference measured as 36.2 °C. A low  $T_g$  is tied to the SebCC phase of the composition, as NIPUs made from lignin alone as cyclocarbonate demonstrated much higher glass transition behavior.<sup>25</sup> With a  $T_g$  below room temperature, it is easy to explain the higher amount of fatigue demonstrated by the NIPU foams in CFD testing *vs.* the PU reference material. NIPUs containing SebCC had increased molecular motion at the CFD testing conditions (*i.e.* above the  $T_g$ ) and led to a lower stress response under continued compression.

TGA analysis (Fig. 6) revealed a three-step degradation process associated with the major components in the foam composition: SebCC, dimer diamine, and CC lignin; the aromatic component of lignin being the last to decompose. These three weight loss events can be observed in peaks associated with the first derivative of weight loss (DTG) found in Fig. S6. Notably, an increase in the  $T_{d5\%}$  from NIPU A to NIPU C suggests that the initial weight loss event is associated with higher lignin content. This result could be tied to the release of water, tightly bound solvent, or small molecules associated with lignin. DTG results for NIPUs A–C all present a peak at approximately 250 °C, absent in the PU reference foam that did not contain lignin. While all of the  $T_{d5\%}$  values are lower than the PU reference, flexible PU foams are not typically applied in high heat environments and thermal stability up to 200 °C is sufficient for most commodity applications.

### Burn testing

Polyurethane foams are inherently flammable and often require additional flame retardants to meet product-specific flammability standards. Lignin has been explored in the past for its own flame retardant properties, including its high char yield and intumescent properties where the charred layer prevents further

combustion.<sup>65,66</sup> The polyurethane reference had no additional flame retardants added.

From Table 4 it is clear that the lignin-based foams all demonstrated slower burn rates than the PU reference foam during horizontal burn testing (NIPU A). Fig. 7 demonstrates that the burnt lignin-based foams resulted in carbonaceous products, consistent with intumescence and TGA results that reported around 12–16% char yield when degraded in an inert environment (compared to 7.6% char yield for the PU reference, Table 3). The burnt products of the PU foam control resulted in ash that could not be recovered without disintegration. Further, the lignin-based foams also performed better with regards to cotton drip testing. Whereas with the PU reference, cotton fibers placed below the sample ignited from falling material, with the lignin-based foams this was not the case. It must be noted that the afterburn time of lignin-based foams was higher than the PU reference, but this can be explained by its overall lower burn rate that would require more time to consume the sample. NIPU C can be considered somewhat as an outlier, as its density is slightly outside of the 250 kg m<sup>-3</sup> specification of the standard (ASTM D4986).<sup>52</sup> Burn testing demonstrated the overall better flame retardant properties of lignin-based foams compared to the PU reference, introducing other benefits regarding the safety and sustainability of the novel materials.

## Conclusion

The design of NIPU foams to meet the current use of commercial PUs is challenging. This study demonstrates that lignin can be utilized in high concentrations, adhering to green chemistry principles, to produce foams with many properties comparable to those of conventional foams, while recognizing the need for further improvements in certain areas. Controlling the molecular weight of lignin during the functionalization steps was necessary to improve the cellular morphology and repeatability of the synthetic process. However, impressive properties could be demonstrated using a larger-scale synthetic process producing 2 kg of functionalized lignin. Furthermore, the high lignin content of our NIPU foams provided improved burn resistance compared to traditional polyurethane foam without flame retardants. A challenge not addressed in this study is the need for heat to cure the foams, whereas traditional PU foams cure at room temperature. Future studies will focus on finding a room temperature curing process that would increase the commercial applicability of this formulation. However, the results reported here present a unique path to low-density, flexible foams that are typically considered out-of-reach for lignin-based products.



## Conflicts of interest

There are no conflicts to declare.

## Data availability

Data supporting this article has been made available in the supplementary information (SI). Supplementary information: additional data for molecular weight of precursors, NMR spectra, rheology data, and derivative thermogravimetric data. See DOI: <https://doi.org/10.1039/d5ra05582b>.

## Acknowledgements

Research supported by the U.S. Endowment for Forestry and Communities through the Public-Private Partnership for Nanotechnology (P3Nano) program, under award #23-JV-1111122-046 (Literature Review, Material Synthesis, Gel Permeation Chromatography, FTIR, Thermogravimetric Analysis, Scanning Electron Microscopy and Nuclear Magnetic Resonance studies, Data Analysis), and as part of the AIM for Composites, an Energy Frontier Research Center funded by the U.S. Department of Energy (DOE), Office of Science, Basic Energy Sciences (BES), under award #DE-SC0023389 (Density Measurements, Rheological Studies, NMR, Compression Force Deflection measurement, and Burn Test).

## References

- 1 United Nations, *Consequences from plastic pollution catastrophic, but solutions possible 'if we act now', secretary-general stresses in message on world environment day*, 2023, <https://press.un.org/en/2023/sgsm21818.doc.htm>.
- 2 On the plastics crisis, *Nature Sustainability*, 2023, **6**(10), 1137.
- 3 J. Tickner, K. Geiser and S. Baima, Transitioning the chemical industry: The case for addressing the climate, toxics, and plastics crises, *Environ.: Sci. Policy Sustainable Dev.*, 2021, **63**(6), 4–15.
- 4 D. Bello, C. A. Herrick, T. J. Smith, S. R. Woskie, R. P. Streicher, M. R. Cullen, Y. Liu and C. A. Redlich, Skin exposure to isocyanates: Reasons for concern, *Environ. Health Perspect.*, 2007, **115**(3), 328–335.
- 5 E. Coureau, L. Fontana, C. Lamouroux, C. Péliissier and B. Charbotel, Is isocyanate exposure and occupational asthma still a major occupational health concern? Systematic literature review, *Int. J. Environ. Res. Public Health*, 2021, **18**(24), 13181.
- 6 C. Sayles, N. Finnegan, T. Pike and M. W. Spence, Toluene diisocyanate occupational exposure data in the polyurethane industry (2005–2020): A descriptive summary from an industrial hygiene perspective, *Toxicol. Ind. Health*, 2022, **38**(9), 606–621.
- 7 A. Cornille, S. Dworakowska, D. Bogdal, B. Boutevin and S. Caillol, A new way of creating cellular polyurethane materials: NIPU foams, *Eur. Polym. J.*, 2015, **66**, 129–138.
- 8 M. Ghasemlou, F. Daver, E. P. Ivanova and B. Adhikari, Bio-based routes to synthesize cyclic carbonates and polyamines precursors of non-isocyanate polyurethanes: A review, *Eur. Polym. J.*, 2019, **118**, 668–684.
- 9 G. Coste, C. Negrell and S. Caillol, Cascade (dithio)carbonate ring opening reactions for self-blowing polyhydroxythiourethane foams, *Macromol. Rapid Commun.*, 2022, **43**(13), e2100833.
- 10 A. D. Sarma, S. V. Zubkevich, F. Addiego, D. F. Schmidt, A. S. Shaplov and V. Berthé, Synthesis of high- $T_g$  nonisocyanate polyurethanes via reactive extrusion and their batch foaming, *Macromolecules*, 2024, **57**(7), 3423–3437.
- 11 S. El Khezraji, S. Gonzalez Tomé, S. Thakur, A. El-Houssaine, B. Y. Hicham, M. Raihane, M. A. Lopez-Manchado, R. Verdejo and M. Lahcini, Fast synthesis of crosslinked self-blowing poly(-hydroxythioether) foams by decarboxylative-alkylation of thiols at room temperature, *Eur. Polym. J.*, 2023, **189**, 111960.
- 12 N. S. Purwanto, Y. Chen and J. M. Torkelson, Biobased, reprocessable, self-blown non-isocyanate polyurethane foams: Influence of blowing agent structure and functionality, *Eur. Polym. J.*, 2024, **206**, 112775.
- 13 X. Xi, A. Pizzi, C. Gerardin, H. Lei, X. Chen and S. Amirou, Preparation and evaluation of glucose based non-isocyanate polyurethane self-blowing rigid foams, *Polymers*, 2019, **11**(11), 1802.
- 14 E. Azadeh, X. Chen, A. Pizzi, C. Gerardin, P. Gerardin and H. Essawy, Self-blowing non-isocyanate polyurethane foams based on hydrolysable tannins, *J. Renewable Mater.*, 2022, **10**(12), 3217–3227.
- 15 X. Chen, X. Xi, A. Pizzi, E. Fredon, X. Zhou, J. Li, C. Gerardin and G. Du, Preparation and characterization of condensed tannin non-isocyanate polyurethane (NIPU) rigid foams by ambient temperature blowing, *Polymers*, 2020, **12**(4), 750.
- 16 H. Blattmann, M. Lauth and R. Mülhaupt, Flexible and bio-based nonisocyanate polyurethane (NIPU) foams, *Macromol. Mater. Eng.*, 2016, **301**(8), 944–952.
- 17 J. H. Clark, T. J. Farmer, I. D. V. Ingram, Y. Lie and M. North, Renewable self-blowing non-isocyanate polyurethane foams from lysine and sorbitol, *Eur. J. Org. Chem.*, 2018, (31), 4265–4271.
- 18 X. Chen, J. Li, X. Xi, A. Pizzi, X. Zhou, E. Fredon, G. Du and C. Gerardin, Condensed tannin-glucose-based NIPU bio-foams of improved fire retardancy, *Polym. Degrad. Stab.*, 2020, **175**, 109121.
- 19 D. L. Smith, D. Rodriguez-Melendez, S. M. Cotton, Y. Quan, Q. Wang and J. C. Grunlan, Non-isocyanate polyurethane bio-foam with inherent heat and fire resistance, *Polymers*, 2022, **14**(22), 5019.
- 20 T. Dong, E. Dheressa, M. Wiatrowski, A. P. Pereira, A. Zeller, L. M. L. Laurens and P. T. Pienkos, Assessment of plant and microalgal oil-derived nonisocyanate polyurethane products for potential commercialization, *ACS Sustainable Chem. Eng.*, 2021, **9**(38), 12858–12869.
- 21 Y. Zhao, Q. Zhang, H. Lei, X. Zhou, G. Du, A. Pizzi and X. Xi, Preparation and fire resistance modification on tannin-based non-isocyanate polyurethane (NIPU) rigid foams, *Int. J. Biol. Macromol.*, 2024, **258**(Pt 2), 128994.





- 22 H.-I. Mao, C.-W. Chen, H.-C. Yan and S.-P. Rwei, Synthesis and characteristics of nonisocyanate polyurethane composed of bio-based dimer diamine for supercritical CO<sub>2</sub> foaming applications, *J. Appl. Polym. Sci.*, 2022, **139**(35), e52841.
- 23 P. Singh and R. Kaur, Sustainable xylose-based non-isocyanate polyurethane foams with remarkable fire-retardant properties, *J. Polym. Environ.*, 2023, **31**(2), 743–753.
- 24 E. Azadeh, A. Pizzi, C. Gerardin-Charbonnier and P. Gerardin, Hydrolysable chestnut tannin extract chemical complexity in its reactions for non-isocyanate polyurethanes (NIPU) foams, *J. Renewable Mater.*, 2023, **11**(6), 2823–2848.
- 25 J. Sternberg and S. Pilla, Materials for the biorefinery: high bio-content, shape memory kraft lignin-derived non-isocyanate polyurethane foams using a non-toxic protocol, *Green Chem.*, 2020, **22**(2), 6922–6935.
- 26 T. Vlcek, U. Cabulis and M. Holynska, Eco-friendlier and non-isocyanate-based polyurethane materials for space applications, *CEAS Space J.*, 2023, **15**(1), 253–264.
- 27 X. Xi, G. Pizzi and G. Du, Glucose-biobased non-isocyanate polyurethane rigid foams, *J. Renewable Mater.*, 2019, **7**(3), 301–312.
- 28 X. Xi, A. Pizzi, H. Lei, G. Du, X. Zhou and Y. Lin, Characterization and preparation of furanic-glyoxal foams, *Polymers*, 2020, **12**(3), 692.
- 29 M. Bourguignon, B. Grignard and C. Detrembleur, Water-induced self-blown non-isocyanate polyurethane foams, *Angew. Chem., Int. Ed.*, 2022, **61**(51), e202213422.
- 30 G. Coste, D. Berne, L. Vincent, C. Negrell and S. Caillol, Non-isocyanate polyurethane foams based on six-membered cyclic carbonates, *Eur. Polym. J.*, 2022, **176**, 111392.
- 31 V. Vincent, N. Kébir, F. Burel and L. Lecamp, Design of biobased non-isocyanate polyurethane (NIPU) foams blown with water and/or ethanol, *EXPRESS Polym. Lett.*, 2023, **17**(9), 974–990.
- 32 N. S. Purwanto, Y. Chen and J. M. Torkelson, Reprocessable, bio-based, self-blowing non-isocyanate polyurethane network foams from cashew nutshell liquid, *ACS Appl. Polym. Mater.*, 2023, **5**(8), 6651–6661.
- 33 N. S. Purwanto, Y. Chen, T. Wang and J. M. Torkelson, Rapidly synthesized, self-blowing, non-isocyanate polyurethane network foams with reprocessing to bulk networks via hydroxyurethane dynamic chemistry, *Polymer*, 2023, **272**, 125858.
- 34 T. Wang, H. Deng, H. Zeng, J. Shen, F. Xie and C. Zhang, Self-blowing non-isocyanate polyurethane foams from cyclic carbonate linseed oil, *ACS Sustainable Resour. Manage.*, 2024, **1**(3), 462–470.
- 35 V. Valette, N. Kébir, F. B. Tiavarison, F. Burel and L. Lecamp, Preparation of flexible biobased non-isocyanate polyurethane (NIPU) foams using the transurethanization approach, *React. Funct. Polym.*, 2022, **181**, 105416.
- 36 F. Monie, B. Grignard, J.-M. Thomassin, R. Mereau, T. Tassaing, C. Jerome and C. Detrembleur, Chemo- and regioselective additions of nucleophiles to cyclic carbonates for the preparation of self-blowing non-isocyanate polyurethane foams, *Angew. Chem., Int. Ed.*, 2020, **59**(39), 17033–17041.
- 37 I. Izarra, A. M. Borreguero, I. Garrido, J. F. Rodríguez and M. Carmona, Comparison of flexible polyurethane foams properties from different polymer polyether polyols, *Polym. Test.*, 2021, **100**, 107268.
- 38 A. Gondaliya and M. Nejad, Lignin as a partial polyol replacement in polyurethane flexible foam, *Molecules*, 2021, **26**(8), 2302.
- 39 M. Bourguignon, B. Grignard and C. Detrembleur, Cascade exotherms for rapidly producing hybrid nonisocyanate polyurethane foams from room temperature formulations, *J. Am. Chem. Soc.*, 2024, **146**(1), 988–1000.
- 40 M. Makarov, M. Bourguignon, B. Grignard and C. Detrembleur, Advancing non-isocyanate polyurethane foams: exo-vinylene cyclic carbonate–amine chemistry enabling room-temperature reactivity and fast self-blowing, *Macromolecules*, 2025, **58**(3), 1673–1685.
- 41 M. Chaib, S. Thakur, H. Ben Youcef, M. Lahcini and R. Verdejo, Achieving rapid foaming in self-blown non-isocyanate polyurethane foams via controlled epoxy functionality in cyclic carbonates, *Eur. Polym. J.*, 2025, **229**, 113843.
- 42 T. Li and S. Takkellapati, The current and emerging sources of technical lignins and their applications, *Biofuels, Bioprod. Biorefin.*, 2018, **12**(5), 756–787.
- 43 G. Henriksson, U. Germgård and M. E. Lindström, A review on chemical mechanisms of kraft pulping, *Nord. Pulp Pap. Res. J.*, 2024, **39**(3), 297–311.
- 44 J. Sternberg, O. Sequerth and S. Pilla, Structure-property relationships in flexible and rigid lignin-derived polyurethane foams: A review, *Mater. Today Sustainability*, 2024, **25**, 100643.
- 45 H. Haridevan, D. A. C. Evans, A. J. Ragauskas, D. J. Martin and P. K. Annamalai, Valorisation of technical lignin in rigid polyurethane foam: a critical evaluation on trends, guidelines and future perspectives, *Green Chem.*, 2021, **23**, 8725–8753.
- 46 D. Trojanowska, F. Monie, G. Perotto, A. Athanassiou, B. Grignard, E. Grau, T. Vidil, H. Cramail and C. Detrembleur, Valorization of waste biomass for the fabrication of isocyanate-free polyurethane foams, *Green Chem.*, 2024, **26**, 8383–8394.
- 47 J. Li, X. Xu, X. Ma, M. Cui, X. Wang, J. Chen, J. Zhu and J. Chen, Antimicrobial nonisocyanate polyurethane foam derived from lignin for wound healing, *ACS Appl. Bio Mater.*, 2024, **7**(2), 1301–1310.
- 48 G. Gellerstedt, Softwood kraft lignin: Raw material for the future, *Ind. Crops Prod.*, 2015, **77**, 845–854.
- 49 G. Rokicki, P. Rakoczy, P. Parzuchowski and M. Sobiecki, Hyperbranched aliphatic polyethers obtained from environmentally benign monomer: glycerol carbonate, *Green Chem.*, 2005, **7**, 529–539.
- 50 C. Carré, L. Bonnet and L. Avérous, Original biobased nonisocyanate polyurethanes: solvent- and catalyst-free synthesis, thermal properties and rheological behaviour, *RSC Adv.*, 2014, **4**(96), 54018–54025.





- 51 D3574 standard test methods for flexible cellular materials—slab, bonded, and molded urethane foams, 2017.
- 52 D4986 standard test method for horizontal burning characteristics of cellular polymeric materials, 2022.
- 53 A. Granata and D. S. Argyropoulos, *J. Agric. Food Chem.*, 1995, **43**(6), 1538–1544.
- 54 G. Tindall, B. Lynn, C. Fitzgerald, L. Valladares, Z. Pittman, V. Bécsy-Jakab, D. Hodge and M. Thies, Ultraclean hybrid poplar lignins via liquid–liquid fractionation using ethanol–water solutions, *MRS Commun.*, 2021, **11**(5), 692–698.
- 55 S. Bair, T. Yamaguchi, L. Brouwer, H. Schwarze, P. Vergne and G. Poll, Oscillatory and steady shear viscosity: The Cox–Merz rule, superposition, and application to EHL friction, *Tribol. Int.*, 2014, **79**, 126–131.
- 56 H. Haridevan, D. A. C. Evans, A. J. Ragauskas, D. J. Martin and P. K. Annamalai, Valorisation of technical lignin in rigid polyurethane foam: a critical evaluation on trends, guidelines and future perspectives, *Green Chem.*, 2021, **23**(22), 8725–8753.
- 57 C. Duval, N. Kébir, R. Jauseau and F. Burel, Organocatalytic synthesis of novel renewable non-isocyanate polyhydroxyurethanes, *J. Polym. Sci., Part A: Polym. Chem.*, 2016, **54**(6), 758–764.
- 58 J. Peyrton and L. Avérous, Structure-properties relationships of cellular materials from biobased polyurethane foams, *Mater. Sci. Eng., R*, 2021, **145**, 100608.
- 59 A. Cornille, C. Guillet, S. Benyahya, C. Negrell, B. Boutevin and S. Caillol, Room temperature flexible isocyanate-free polyurethane foams, *Eur. Polym. J.*, 2016, **84**, 873–888.
- 60 C. Casavola, L. D. Core, V. Moramarco, G. Pappaletta and M. Patronelli, Experimental and numerical analysis of the Poisson's ratio on soft polyurethane foams under tensile and cyclic compression load, *Mech. Adv. Mater. Struct.*, 2022, **29**(28), 7172–7188.
- 61 L.-Y. Liu, M. J. Cho, N. Sathitsuksanoh, S. Chowdhury and S. Renneckar, Uniform chemical functionality of technical lignin using ethylene carbonate for hydroxyethylation and subsequent greener esterification, *ACS Sustainable Chem. Eng.*, 2018, **6**(9), 12251–12260.
- 62 A. Duval and L. Avérous, Cyclic carbonates as safe and versatile etherifying reagents for the functionalization of lignins and tannins, *ACS Sustainable Chem. Eng.*, 2017, **5**(8), 7334–7343.
- 63 I. Kühnel, B. Saake and R. Lehen, A new environmentally friendly approach to lignin-based cyclic carbonates, *Macromol. Chem. Phys.*, 2018, **219**(7), 1700613.
- 64 A. Duval, W. Benali and L. Avérous, Turning lignin into a recyclable bioresource: transesterification vitrimers from lignins modified with ethylene carbonate, *Green Chem.*, 2024, **26**, 8414–8427.
- 65 N. N. Solihat, A. F. Hidayat, M. N. A. M. Taib, M. H. Hussin, S. H. Lee, M. A. A. Ghani, S. S. A. O. Al Edrus, H. Vahabi and W. Fatriasari, Recent developments in flame-retardant lignin-based biocomposite: Manufacturing, and characterization, *J. Polym. Environ.*, 2022, **30**(11), 4517–4537.
- 66 V. Muir, N. Tripathi, A. Rodriguez-Urbe, A. K. Mohanty and M. Misra, Sustainable biocomposites from pyrolyzed lignin and recycled nylon 6 with enhanced flame retardant behavior: Studies on manufacturing and quality performance evaluation, *SPE Polym.*, 2024, **5**, 277–292.

